

Supporting Information for

A multifunction phenylphosphinamide additive for stable flexible inverted perovskite solar cells

Feihu Liu, Jidong Geng, Wei Zhang, Jie Dou,* Qiyao Guo, Jialong Duan and Qunwei Tang *

Institute of Carton Neutrality, College of Chemical and Biological Engineering, Shandong University of Science and Technology, Qingdao 266590, PR China.

Experimental

Materials

All the commercial materials were used as received without any future purification, including Lead iodide (PbI_2 , 99.99%, Xi'an Polymer Light Technology Corp.), lead bromide (PbBr_2 , 99.99%, Xi'an Polymer Light Technology Corp.), Cesium Iodide (CsI , 99.9%, Sigma-Aldrich), Formamidinium iodide (FAI, greatcell solar), methylammonium iodide (MAI, greatcell solar), Methylammonium bromide (MABr, greatcell solar), Methylamine hydrochloride (MACI, greatcell solar), anhydrous N, N-dimethylformamide (DMF, 99.99%, Sigma-Aldrich), Dimethylsulfoxide (DMSO, 99.99%, Sigma-Aldrich), Isopropyl alcohol (99.9%, aladdin), [2-(3,6-Dimethoxy-9H-carbazol-9-yl)ethyl]phosphonic Acid (MeO-2PAcz, TCI), [6,6]-Phenyl C61 butyric acid methyl ester (PC61BM, 99.5%, Xi'an Polymer Light Technology Corp.), 2,9-dimethyl-4,7-diphenyl-1,10-Phenanthroline (BCP, 99% Xi'an Polymer Light Technology Corp.), [2-(9H-Carbazol-9-yl)ethyl]phosphonic acid (98%, TCI), P,P-Diphenylphosphinic amide (DPPA, 99%, aladdin), Nickel oxide (NiO_x , 99.99%, aladdin), Etanol (99.9%, aladdin), Chlorobenzene (99.99%, Sigma-Aldrich), and PEN substrate (PECCELL).

Device fabrication

Preparation of hole/electron transport solution: the PEN substrate was cleared with deionized (DI) water, ethanol, respectively. The NiO_x solution was prepared by dissolving 10 mg NiO_x in 1 mL of H_2O . The MeO-2PAcz solution

was prepared by dissolving 10 mg MeO-2PACz in 1 mL of Etanol. The PC61BM solution was prepared by dissolving 20 mg PC61BM in 1 mL of Chlorobenzene. The BCP solution was prepared by dissolving 0.5 mg BCP in 1 mL of isopropyl alcohol.

Preparation of pristine and molecule-doped perovskite precursor solution: 6.7mg MABr, 8.8 mg MAcl, 18.2 mg CsI, 196.1 mg FAI, 22 mg PbBr₂ and 572 mg Pbl₂ were dissolved in 865 μ l DMF and DMSO solution (volume ratio 4:1) and stirred at 60 °C for 1 h to prepare undoped precursor solution. For doped solution, another 0.5~2 mg DPPA was added in the preceding solution.

*Device fabrication:*The NiO_x layer was formed by spin-coating the precursor solution at 3000 rpm for 30 s and then short-baking at 120 °C for 20 min in the air. The MeO-2PACz was formed by spin-coating the precursor solution at 3000 rpm for 30 s and then short-baking at 100 °C for 10 min in the air. The as-prepared perovskite precursor solution was spin-coated onto the hole transport substrate with speed of 1000 rpm for 5 s and 4000 rpm for 30 s. During the last 15 s of the spinning process, the liquid film was treated by drop-casting chlorobenzene solvent (150 μ l). The substrates were annealed on a hot plate at 100°C for 50 min.The PC61BM layer was formed by spin-coating the precursor solution at 1500 rpm for 30 s and then short-baking at 100 °C for 1 min in the N₂ atmosphere. The BCP layer was formed by spin-coating the precursor solution at 1500 rpm for 30 s and then short-baking at 100 °C for 1 min in the N₂ atmosphere. Finally, 100 nm thick of Cu was deposited on top by thermal evaporation. The active area of PSCs is 0.03725 cm² as determined by the mask.


Characterizations

Fourier transform infrared (FTIR) spectra were performed by the infrared spectrometer (Bruker TENSOR-27). The X-ray photoelectron spectroscopy (XPS) studies were performed using a Thermo-VG Scientific ESCALAB 250 photoelectron spectrometer equipped with a monochromated Al Ka (1486.6 eV) X-ray source. The composition was characterized by X-ray diffraction (Rigaku, with Cu-K α radiation of $\lambda=0.15418$ nm). Photoluminescence (PL)

and time-resolved photoluminescence (TRPL) were measured by FLS980 (Edinburgh Instruments Ltd) with an excitation at 470 nm. Spectroscopy (UPS) measurements were carried out on an XPS AXIS Ultra DLD (Kratos Analytical). The absorption spectra measurement was analyzed by UV-vis spectroscopy (SHIMADZU, UV-2600). The 2D photoluminescence (PL) map was executed by A Laser Scanning Confocal Microscope (Enlitech, SPCM-1000) equipped with an 470 pulse laser and a galvo-based scanner. Depth-resolved GIXRD was characterized through the Rigaku Smart Lab five-axis X-ray diffractometer at 45 kV and 200 mA, equipped with Cu α radiation ($\lambda = 1.54050 \text{ \AA}$), parallel beam optics, and a secondary graphite monochromator. For the residual stress tests, a slow scan rate of $0.15 \text{ }^\circ \text{min}^{-1}$ was carried out to ensure fine structural information. The scanning electron microscopy was measured via a scanning electron microscope (Hitachi S8230).

The photovoltaic performance of the PSCs was collected with a source meter (Keithley 2400), the light source (SS-F5-3A, Enlitech) by reverse scanning from 1.2 to -0.2 V or forward scanning from -0.2 to 1.2 V at a scanning speed of 50 mV s^{-1} and quantum efficiency measurement system (QE-R, Enlitech). The ideality factor α was obtained by the related equation : $V_{oc} = \alpha \frac{k_B T}{e} \ln\left(\frac{I_0}{I_L}\right) - \frac{E_g}{e}$ where n is the ideality factor, k_B is the Boltzmann constant, e is the elementary charge, T is the absolute temperature, and I is the light intensity. The illumination stability of devices was executed under one sun-equivalent white. For the open-circuit photo-thermal stability test, the devices were kept under an array of white LEDs with one-sun intensity (100 mW/cm^2) in an N_2 glove box. The average temperature was kept at $\sim 45 \text{ }^\circ \text{C}$. Then, all devices were taken out from the chamber and tested at different time intervals under a separate solar simulator (AM 1.5G, 100 mW/cm^2) for $J-V$ characterization. The device MPP tracking was measured with a CHI 1000C potentiostat under the white LED lamp (100 mW/cm^2) in an N_2 glove box. Then, the devices were measured with a maximum power point (MPP) tracking routine under continuous illumination. The MPP was updated every 300 s by a standard perturb and observation method. The average temperature was kept at $\sim 45 \text{ }^\circ \text{C}$. The repeated bending cycle tests are performed by a custom-made

stretching machine, which is actuated by a stepper motor (Shenzhen RUPI Materials). All devices were taken out from the chamber and tested under a separate solar simulator (AM 1.5G, 100 mW/cm²) for J–V characterization.

-6.871e-2  6.871e-2

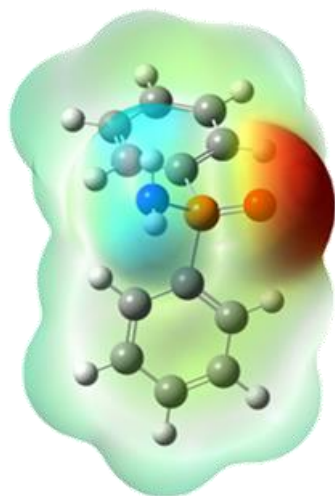


Figure S1 ESP map of DPPA molecules.

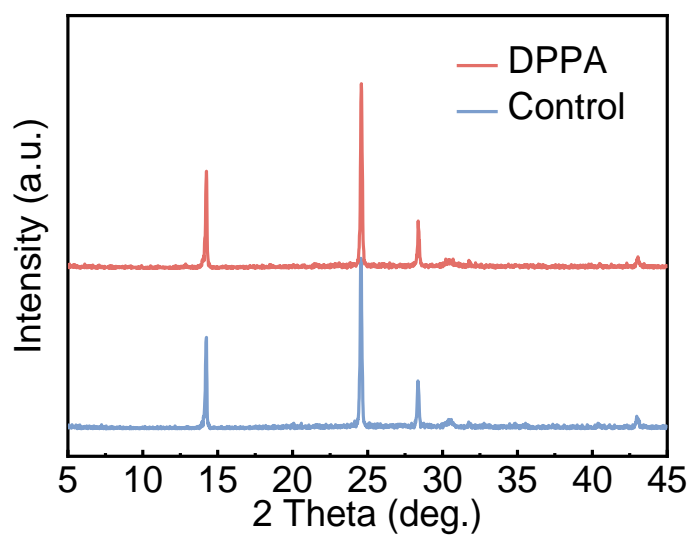


Figure S2 The XRD patterns of the perovskite and DPPA doped perovskite films.

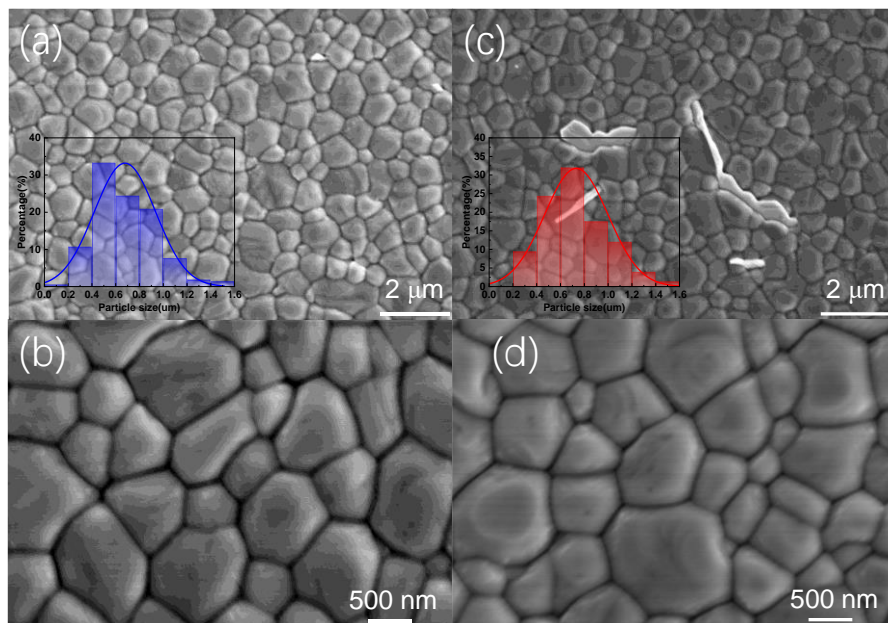


Figure S3 The Top-view SEM images and particle size distribution maps of the (a, b) perovskite and (c, d) DPPA doped perovskite films.

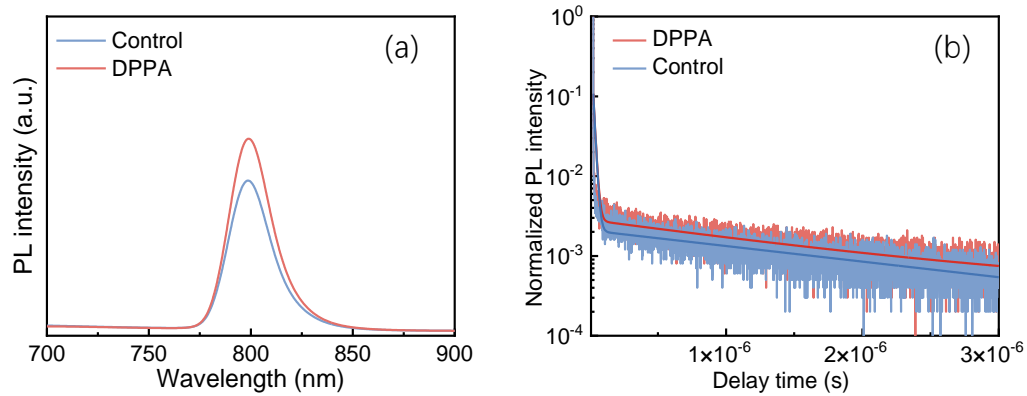


Figure S4 (a) The steady-state PL spectroscopy of the perovskite/glass film with and without DPPA treatment (b) the time-resolved decay spectra of the perovskite/glass without and with ZIF-67 DPPA.

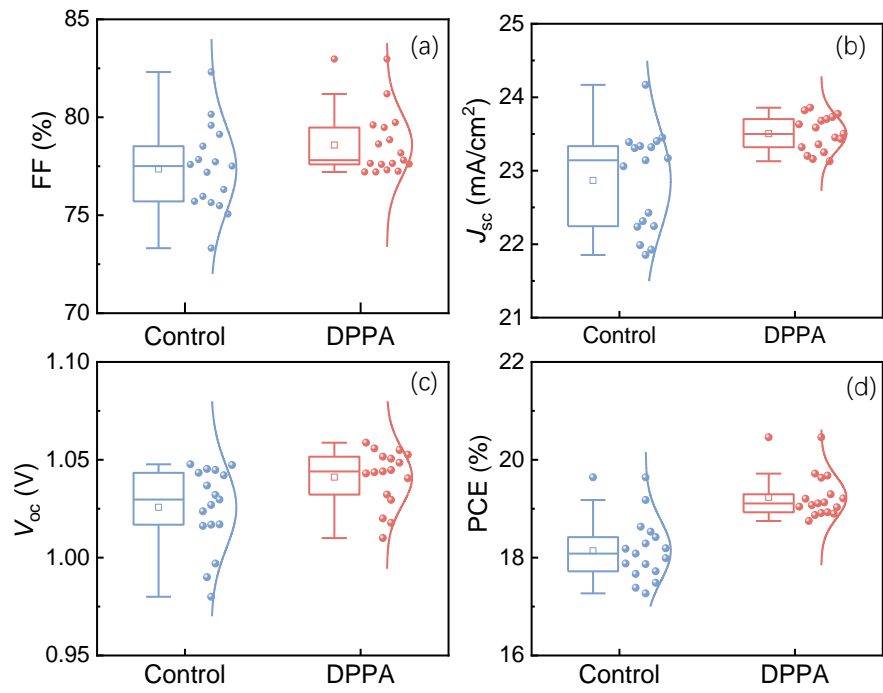


Figure S5 Box charts of photovoltaic parameters of (a) J_{sc} , (b) V_{oc} , (c) FF and, (d) PCE extracted from J-V measurements for the PSCs without and with DPPA treatment, respectively.

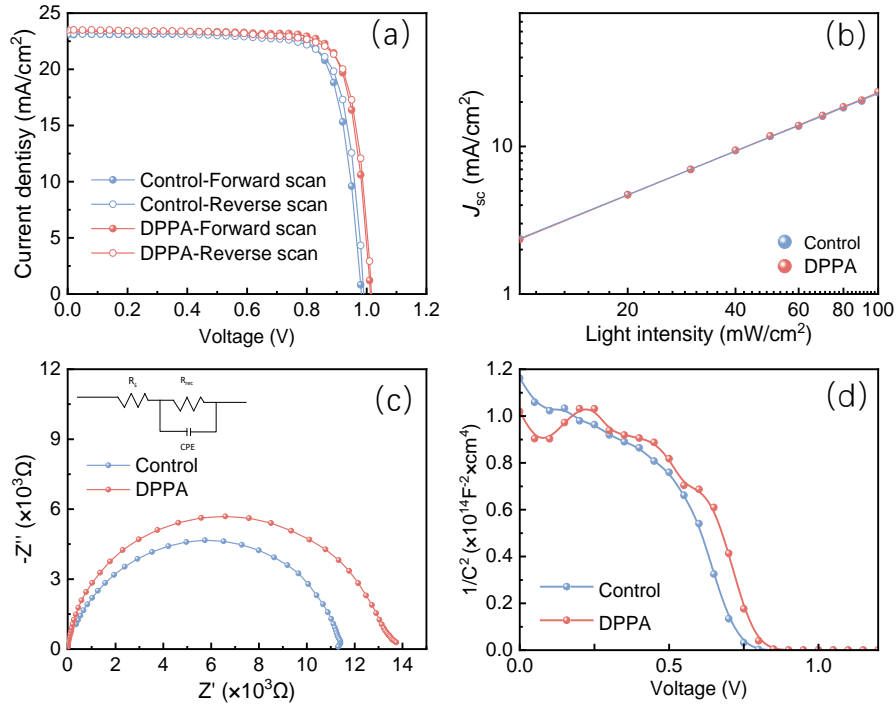


Figure S6 (a) J–V curves of the PSCs without and with DPPA treatment measured by forward and reverse scan; (b) J_{sc} upon light intensity modulated J–V measurements; (c) EIS plots; (d) M–S plots of the PSCs without and with DPPA treatment.

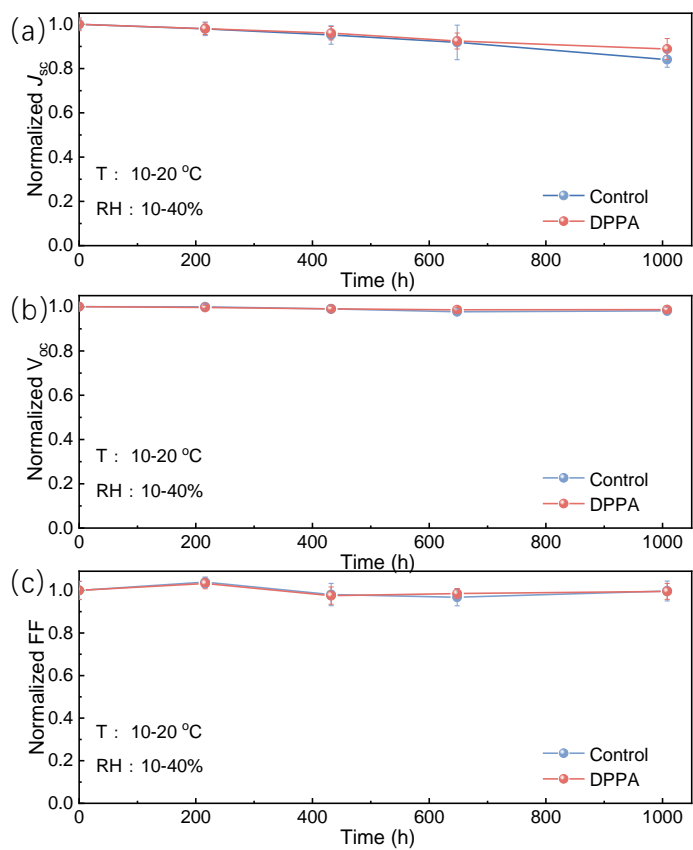


Figure S7 Photovoltaic performance parameters: (a) J_{sc} , (b) V_{oc} , and (c) FF of devices in the air environment.

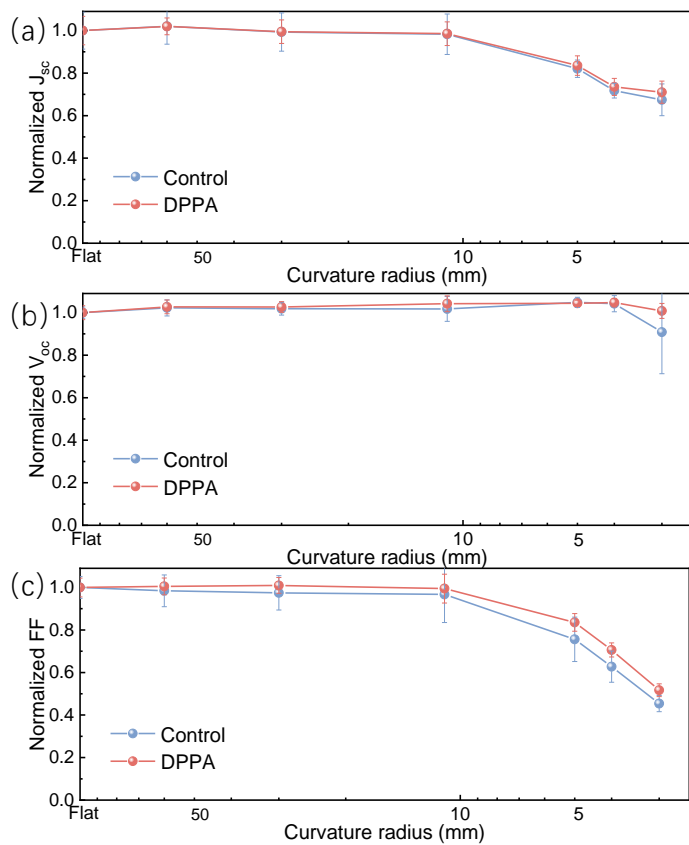


Figure S8 Photovoltaic performance parameters: (a) J_{sc} , (b) V_{oc} , and (c) FF of flexible devices under bending 1 cycle with different bending radii.

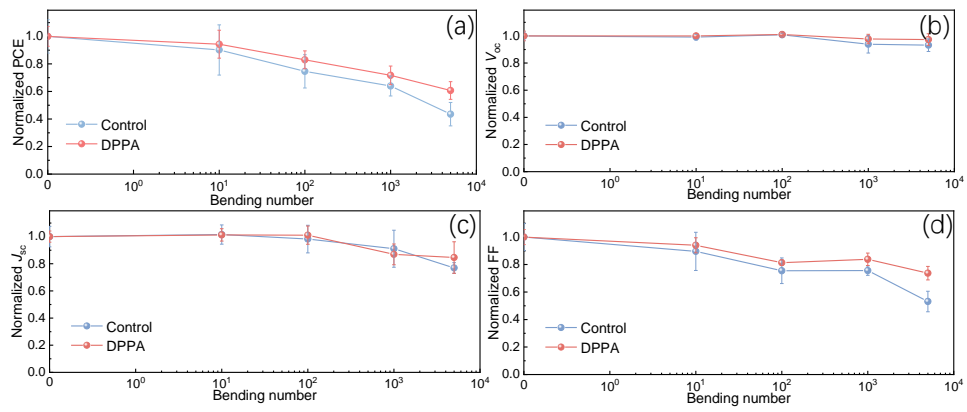


Figure S9 Photovoltaic performance: (a) PCE, (b) V_{oc} , (c) J_{sc} , and (d) FF of flexible devices under bending cycles with a radius of 10 mm.

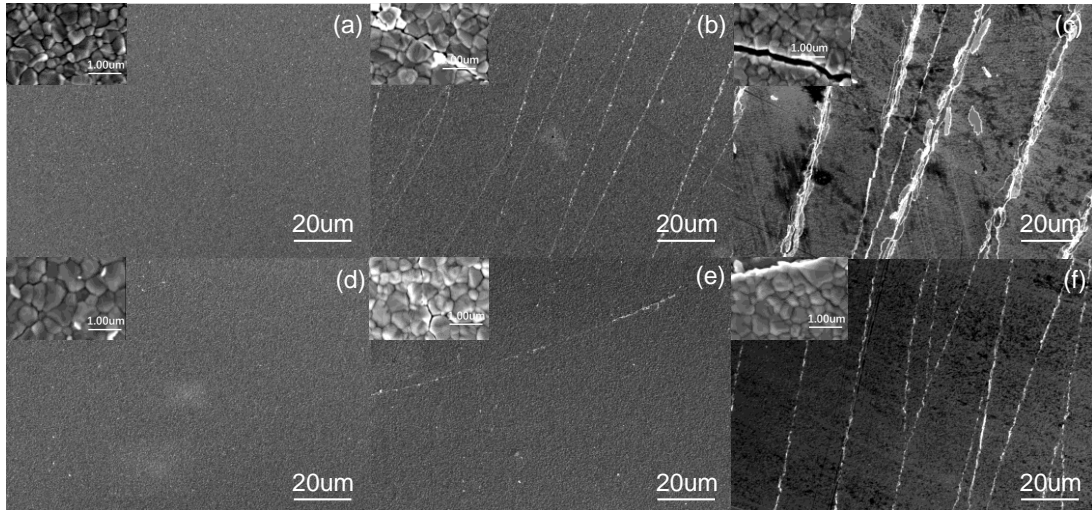


Figure S10 SEM images of flexible perovskite films (a-d) without and (e-h) with DPPA treatment after bending test.

Table S1 Those champion device performance parameters of the control and DPPA treated device.

Concentration	V_{oc} (V)	Efficiency (%)	Fill Factor (%)	J_{sc} (mA/cm ²)
0	1.017	19.64	82.31	23.45
0.05	1.029	20.41	83.31	23.80
0.1	1.043	20.46	82.97	23.63
0.2	1.018	19.68	82.69	23.38

Table S2 Those device performance parameters of the control and DPPA treated device measured by forward and reverse scan.

Devices	V_{oc} (V)	Efficiency (%)	Fill Factor (%)	J_{sc} (mA/cm ²)
Control-Forward scan	0.98	18.11	80.15	23.06
Control-Reverse scan	0.99	18.19	79.13	23.17
DPPA-Forward scan	1.01	19.12	81.19	23.32
DPPA-Reverse scan	1.02	19.08	79.60	23.50